THE ASTROPHYSICAL JOURNAL SUPPLEMENT SERIES, 107:255–262, 1996 November

AN ATLAS OF ANCIENT PLANETARY NEBULAE AND THEIR INTERACTION WITH THE INTERSTELLAR MEDIUM[1]

RICHARD W. TWEEDY[2]
Steward Observatory, University of Arizona, Tucson, AZ 85721; tweedy@as.arizona.edu
AND
KAREN B. KWITTER
Department of Astronomy, Williams College, Williamstown, MA 01267; kkwitter@williams.edu
Received 1995 July 21; accepted 1996 May 16

ABSTRACT

We present an imaging atlas of the largest planetary nebulae (>8′), taken at Hα, [N II], and [O III]. Using this data, we have developed a set of simple criteria for determining whether a planetary nebula (PN) is indeed interacting with the interstellar medium (ISM). On this basis, we conclude that most in our sample reveal significant interactions with the ISM. We discuss also how a large sample of ancient planetary nebulae can be used to derive a filling factor for coronal gas in the ISM.

Subject headings: atlases — ISM: structure — planetary nebulae: general

1. INTRODUCTION

Planetary nebulae supply about 1 $M_\odot$ of material per year to the interstellar medium (ISM). While many studies have investigated the early stages in the lives of planetary nebulae, when they are young, bright, and rather symmetric (e.g., Balick 1987; Frank & Mellema 1994; Mellema 1993), little has been done on the late stages, when the nebulae become significantly affected by the interstellar material with which they will eventually merge. There is a severe paucity of observational data; the pioneering analytical work of Borkowski, Sarazin, & Soker (1990), for example, was based predominantly on inspection of the Palomar Sky Survey (PSS). For this reason, we have observed about 30 ancient planetary nebulae at Hα, [N II], and [O III]. Early results have been published on some of the objects elsewhere (Tweedy & Kwitter 1994a, 1994b; Tweedy & Napiwotzki 1994), as well as a thorough investigation of the closest planetary nebula, S216 (Tweedy, Martos, & Noriega-Crespo 1995).

Our main purpose here is to present the new data, but we wish also to provoke theorists to give these objects serious attention. In reviewing the H I in the Galaxy, Dickey & Lockman (1990) commented that "The temperature variations of the interstellar medium are so dramatic, its pressure structure so problematic, and its dynamics, hydrodynamics, and/or magnetohydrodynamics are so intricate that it has commanded the attention of several generations of the finest theoretical astrophysicists." We believe that the use of ancient planetary nebulae to probe the ISM at known locations will enable significant progress to be made in addressing each of these issues. The reason is that not only are the morphologies of these planetary nebulae significantly affected by their surroundings, but so is the ionization structure. In Tweedy & Kwitter (1994a), it was suggested that this ionization effect could be used to infer straightforwardly the density of the surroundings; however, in the study of S216, Tweedy et al. (1995) began to recognize that the ISM is rather complicated and may be dominated more by its magnetic fields than by its density structure. We wish to consider this situation further, while acknowledging that there is no substitute for detailed numerical modeling.

2. OBSERVATIONS AND DATA REDUCTION

The observations reported here were taken on about 20 nights mostly between 1993 March and 1995 June at the Burrell Schmidt telescope on Kitt Peak (see Table 1). This telescope has a 36 inch primary mirror with a 24 inch corrector, providing fast optics of $f/3.5$. Since 1989, it has been equipped with a 2048 × 2048 CCD, on loan from the Space Telescope Science Institute (STScI). The pixel size is 2.″05, leading to a typical FWHM of ≈4″ for the stellar images. There are two narrow bands of hot columns that have been avoided, but apart from this the detector is cosmetically well behaved. Five filters have been used for the observations reported in this paper, of which two ([O III] λ5007 and [S II] λ6725) are owned by the National Optical Astronomy Observatories (NOAO), two (Hα and [N II] λ6584) are owned by K. B. Kwitter and one (also [O III] λ5007) was borrowed from B. Balick of the University of Washington Astronomy Department (see Table 2 for the filter characteristics). The data reduction was performed using standard IRAF procedures. In most cases shown here, single images were taken of each object, in two or three filters. This was believed to be sufficient for the present purposes: namely, to establish gross behavior associated with the interaction of plantery nebulae with the interstellar medium.

3. TARGET SELECTION

The primary source list was taken from Table 2 of Borkowski et al. (1990). This was essentially a list of all those nebulae known to have one axis larger than 8′. A few other nebulae were also observed, whose selection was rather idiosyncratic, and which are discussed separately. Since the Borkowski et al. paper was published, a few other ancient planetary nebulae have been identified: Table 3 below is therefore an updated list. Since the central stars are so important for determining the distances to these objects and their evolutionary ages, the currently determined central star parameters are given in Table 4.

[1] The observations reported here were made with the Burrell Schmidt telescope of the Warner and Swasey Observatory, Case Western Reserve University.
[2] Visiting Astronomer, Kitt Peak National Observatory.

TABLE 1

LOG OF OBSERVATIONS

OBJECT NAME	DATE	EXPOSURE TIMES (sec) Hα	[N II]	[O III]	[S II]
A7	1993 Oct 11	...	600	600	...
A21	1992 Oct 12	1200	...	...	...
A24	1994 Apr 20	600	600	600	...
A29	1994 Apr 20	600	600	600	...
A35	1994 Apr 19	600	...	600	...
	1994 Apr 20	...	600	...	...
A74	1993 Sep 6	...	1200	1200	...
	1993 Oct 14	1800	...	...	...
DHW 5	1995 Jun 6	1200	1200	1200	1200
EGB 6	1994 Apr 7	600	600	600	...
HW4	1994 Nov 24	...	...	900	...
	1994 Nov 26	900	...	...	...
IW 1	1994 Nov 24	1800	900	1800	...
IW 2	1993 Sep 7	1800	1800	...	...
Jacoby 1	1994 Apr 5	1800	1800	1200	...
MWP 1	1993 Sep 5	1200	1200	1800	...
PW 1	1993 Oct 10	900	...	900	...
	1993 Oct 11	...	900	...	...
S68	1995 Jun 1	900	900	...	...
S78	1995 May 29	...	1800	...	...
	1995 May 30	1800	...	...	...
	1995 Jun 4	...	...	1800	...
S176	1993 Sep 5	...	1200	...	...
	1993 Sep 6	1200	...	1200	...
S188	1993 Sep 7	1800	600	1800	...
WDHS 1	1993 Mar 16	600	...	...	...
	1993 Oct 11	...	600	600	...

We used apparent diameter as an expedient method of selection, but it is one that happens to be highly effective for our current purposes. It may be objected that a planetary nebula that is apparently large could be a young object nearby, or an older one farther away. However, if the central star characteristics in Table 4 are examined, it will be seen that all those listed are close to becoming, or are already, white dwarfs, thus testifying to their advanced age. Therefore, the planetay nebulae with the largest apparent sizes are both nearby and old. However, five of the total sample of 27 are not interacting with the ISM, and of these, three are found among the six smallest; we doubt whether our expediency can be stretched much beyond our current sample.

An important question remains unanswered, however: how many of the identifiable ancient planetary nebulae have actually been detected? Many in Table 3 were originally discovered on the Palomar Sky Survey (PSS) by the Innsbruck group, led by R. Weinberger. However, the sensitivity of the plates is known to vary substantially, and very faint nebulae such as IW 1 and 2 would not have been detected with plates of more normal sensitivity. Other methods have been used to detect faint nebulae, with several searches having been done around known hot white dwarfs (e.g., Kwitter et al. 1989; Motch, Werner, & Pakull 1993; Tweedy & Kwitter 1994b; Jacoby & van de Steene 1995). It is perhaps reassuring that the two brightest new nebulae (MWP 1 and Jacoby 1) are strong emitters of [O III] λ5007: on the PSS blue plate, this wavelength had a sensitivity a factor of 8 below the peak, whereas both Hα and [N II] occur at wavelengths close to the peak sensitivity of the red plate. Both nebulae have exceptionally hot central stars. Two other new nebulae are very faint arcs near two hot H-rich white dwarfs, which are probably the oldest planetary nebulae so far detected. Both were well below the limit of the PSS.

4. CRITERIA FOR DETERMINING WHETHER A PN IS INTERACTING WITH THE ISM

S216 is a classic example of the interaction of a PN with the ISM, since it exhibits all the characteristics expected for a fairly advanced interaction. In particular, the white dwarf is substantially displaced with respect to the center of the nebula, toward a region of enhanced emission which also has a lower ionization level. However, the interaction between a PN and the ISM will occur before the central star is obviously displaced, so that it is desirable to be able to identify these nebulae in which this is occurring.

We have argued elsewhere that the drop in the ionization level in the interaction region is a crucial characteristic (Tweedy & Kwitter 1994a). However, we have come to realize that while this is a necessary consequence of the interaction, it is not a sufficient criterion for identifying it. A drop in ionization will take place when the nebula expands beyond its Strömgren zone, which it will do even without an interaction with the ISM to boost the recombination rate: this was discussed for S216 in Tweedy et al. (1995) and is exemplified nicely here by Abell 74, where the O^{++} zone is restricted to a region close to the central star. Second, a similar drop may also occur in localized regions well within the nebula. Such regions in younger nebulae include the ansae; e.g., NGC 3242 and NGC 7662 (Balick et al. 1993); and similar features are present in Abells 7 and 31. Abell 7 is a particularly pertinent example: the images presented here might in themselves be suggestive of localized patches of PN-ISM interaction, but an astonishingly detailed [O III] image produced by G. Jacoby shows a large halo of material beyond these patches which must instead be formed well within the nebula. Similar features do appear in Abell 31, which does appear to be interacting with the ISM as well.

The criteria that we have come up with so far are as

TABLE 2

FILTER CHARACTERISTICS

Filter	Peak Wavelength (Å)	Throughput at line (%)	FWHM (Å)	Notes
Hα (KBK)	6563	48	19	0.1% at [N II] 6584 Å; 20% at [N II] 6548 Å
[N II] λ6584 (KBK)	6588	46	20	5% at Hα
[O III] (NOAO)	5014	63	53	
[O III] (BB)	5016	76	60	
[S II] (NOAO)	6733	85	84	Same for 6717 and 6731 Å

TABLE 3

LARGE PLANETARY NEBULAE: AN UPDATED LIST

Name	Galactic Coordinates (PN G)	Angular Size (arcmin)	Linear Size (pc)	ISM Interaction?	Morphological Class	Figure Number or Reference for Images
S216	158.6+00.7	100 × 100	3.0 × 3.0	Yes	Ff	Tweedy et al. 1995
RE 1738+665	96.9+32.0	~ 60	~ 4.0	Yes	Cf	Tweedy & Kwitter 1994b
Ton 320	191.4+33.1	~ 30	~ 4.0	Yes	Cf	Tweedy & Kwitter 1994b
WDHS 1	197.4−06.4	22 × 17	6.4 × 5.0	Yes	S	Fig. 1
PW 1	158.9+17.8	20 × 20	1.9 × 1.9	Yes	Ff	Fig. 2
NGC 7293	036.1−57.1	18 × 18	1.6 × 1.6	Halo	H	Kwitter et al. 1996
Abell 31	219.1+31.2	17 × 16	7.6 × 7.1	Yes	F	Tweedy & Kwitter 1994a
IW 2	107.7+07.8	16 × 14	6.9 × 6.1	Yes	Sf	Fig. 1
Abell 35	303.6+40.0	16 × 11	1.6 × 1.1	Yes	...	Fig. 3
HFG 1	136.5+05.5	15 × 15	1.5 × 1.5	Yes	F	Heckathorn et al. 1982
Abell 74	072.7−17.1	15 × 13	4.9 × 4.2	Yes	F	Fig. 4
NGC 6853	060.8−03.6	15 × 12	1.5 × 1.2	Halo	H	Kwitter et al. 1996
Abell 7	215.5−30.8	15 × 11	4.0 × 3.0	No	...	Fig. 10
S174	120.3−18.3	15 × 10	2.0 × 1.2	Yes	S	Tweedy & Napiwotzki 1994
MWP 1	80.8−10.6	13 × 9	5.3 × 3.7	Yes	B	Fig. 5
IW 1	149.7−03.3	13 × 13	1.8 × 1.8	Yes	F	Fig. 6
S176	120.2−05.3	13 × 11	1.0 × 0.8	Yes	Ff	Fig. 6
EGB 6	221.6+46.4	13 × 11	1.7 × 1.5	Yes	F	Fig. 7
Abell 21	205.1+14.2	12 × 9	1.2 × 0.9	Yes	Cf	Fig. 8
Jacoby 1	85.4+46.4	11 × 11	3.2 × 3.2	Yes	F	Fig. 7
S78	46.0+03.0	11 × 9	4.5 × 3.7	Yes	Ff	Fig. 8
LT 5	339.0+88.0	9 × 8	1.1 × 1.0	No	...	Longmore & Trition 1980
HW 4	149.0−09.0	9 × 9	1.0 × 1.0	Yes	C	Fig. 12
S188	128.0−04.1	9 × 8	1.5 × 1.4	Yes	Cf	Fig. 9
DHW 5	111.0+11.6	9 × 9	1.2 × 1.2	Yes	Cf	Fig. 11
Abell 29	244.0+12.0	8 × 6	1.0 × 0.7	No	...	Fig. 10
Abell 36	318.4+41.5	8 × 5	1.4 × 0.8	No	...	...

follows:

1. The outer regions of the nebulae are asymmetric;
2. There is a flux enhancement located at a distinct edge, in the outer regions of the nebula;
3. This is accompanied by a drop in the ionization level.

These three taken together appear to be sufficient, and we have not come across a case in which such an edge occurs without the corresponding ionization effect. All nebulae in which we have observed distinct edges also reveal diffuse edges, which are often downstream from the presumed PN-ISM interaction.

TABLE 4

CENTRAL STAR CHARACTERISTICS

Name	V	$T_{\rm eff}$	log g	Distance	z	Class
S216	12.66	81,000	6.9	120	1.5	DAO
RE 1738+665	14.64	88,000	7.5	220	117	DA
Ton 320	15.82	70,000	7.7	440	240	DAO
WDHS 1	17.4	220,000	7.4	1000	−111	DA
PW 1	15.3	62,000	7.0	320	98	DAO
NGC 7293	13.43	107,000	7.0	300	−252	DAO
Abell 31	15.51	95,000	6.3	1530	800	DAO
IW 2	17.71	...	...	1490	202	DAO
Abell 35	...	...	...	...	...	WD+G
HFG 1	14.5	...	...	...	...	PCB
Abell 74	17.11	66,000	7.0	1120	−330	DAO
NGC 6853	13.94	99,000	6.8	370	−26	DAO
Abell 7	15.44	110,000	6.8	930	−476	DAO
S174	14.74	64,000	6.8	520	−163	DAO+WD
MWP 1	13.16	150,000	6.5	1400	−257	PG 1159
IW 1	16.56	...	...	480	−28	PG 1159
S176	18.7	...	...	>2000	>185	sdO
EGB 6	16.00	70,000	7.5	460	333	DAO
Abell 21	15.99	100,000	7.0	600	147	PG 1159
Jacoby 1	15.9	140,000	7.0	1000	724	PG 1159
S78	17.7	100,000	7.0	1420	74	PG 1159
LT 5	...	...	...	...	...	sd O+G
HW 4	17.0	...	...	400	−63	DAO
S188	17.44	...	...	600	−42	DAO
DHW 5	15.4	82,000	6.8	470	95	DAO
Abell 29	17.0	...	...	...	...	DAO
Abell 36	...	...	...	...	...	sd O+G

5. IS THE PN INTERACTING WITH ISM OR REMNANT AGB MATERIAL?

Although we have hitherto assumed that it is the ISM with which the PN is interacting, it is possible that this interpretation is incorrect. If the red giant envelope was not fully swept up by the time the fast wind from the central star ceased, then the PN may be interacting with this instead. There are a number of considerations that this is not the case, at least for the majority of the nebulae considered here. First, the models computed by Mellema (1993) suggest that most of the asymptotic giant branch (AGB) material is swept up after $\sim$2000 years. Second, this scenario in isolation cannot explain the asymmetries, the outer reaches of AGB wind material tend to be more symmetrical than the inner region in which the young PNe are formed (e.g., Plait & Soker 1990; Soker 1994; Mellema 1993). Thus, the AGB material itself must be interacting with the ISM. Third, the asymmetries that are indicative of interaction with the ISM are sharp edged, which implies a sharp drop in the density; the nebula is thus density bounded, not ionization bounded. Finally, the density beyond the edge must be extremely low, otherwise it would also be lit up by the central star.

Nevertheless, one can think of circumstances in which red giant wind material might play an important role. Central stars of extremely high mass ($>0.8\ M_{\odot}$) are likely candidates for the wind to shut off even within 1000 years (Blöcker & Schönberner 1991). Only one of the central stars considered here is a candidate for such a high mass: although still rather uncertain, the mass of WDHS 1 appears to be in the region of 0.7–0.8 $M_{\odot}$. A curious example is S174, which has a low-mass central star (Tweedy & Napiwotzki 1994), which from observations of other similar stars is expected to be a close binary white dwarf (Holberg et al. 1995). Here the envelope of the red giant was ejected before core He ignition could occur. In this case, the system did not undergo a normal PN phase, so that what appears as the nebula is probably just the unswept red giant envelope.

6. NOTES TO THE TABLES AND ATLAS

Most of the columns in Table 3 (details of the planetary nebulae) and Table 4 (information on the central stars) are self-explanatory. The morphological classification scheme in column (6) is described in § 7. Some of the images of the nebulae have been published elsewhere, and these are indicated by references in column (7). The effective temperatures, surface gravities, and distances have all been taken from the spectral analysis of the Kiel group: for the DA and DAO stars, these are generally from Napiwotzki (1993); for the H-poor PG 1159 stars, these are from Werner (1993), and references therein.

Most of the central stars have been marked on the figures, but the reader should be aware that not all the images are usable as finder charts. In particular, although the locations for those in IW 1 and S188 are marked correctly, in neither case is the star actually visible; this is particularly confusing for IW 1 because the marks in the figure appear to point directly to a star, which is actually just a line-of-sight neighbor. The central star of S78 is also blended with a neighbor. These points are addressed further in § 8.

Many of the images were taken in nonphotometric conditions, so that no detailed attempt has been made to calibrate the images displayed. However, where both [N II] and Hα images show the nebula clearly, they have been placed on a common intensity scale, so that a qualitative feel for the relative strengths can be obtained.

7. EXPLANATION OF CODE FOR APPEARANCE OF PNe INTERACTING WITH ISM

A short code has been given for the appearance of those nebulae that are interacting with the ISM. No designation is therefore given to those like Abell 29 and LT 5, which do not appear to be interacting. It is assumed tacitly that all nebulae interacting with the ISM show an asymmetric enhancement somewhere, with an accompanying ionization drop, so we make no attempt to record this in the code.

1. B type, which indicates a bipolar morphology, occurs in only one nebula, MWP 1. About 10% of younger nebulae are bipolar, so this group is expected to be small.
2. The F type has been given to those nebulae that appear to be uniformly filled, such as Abells 31 and 74. This is inferred in general when there is an [O III] zone present, but which is considerably smaller than the nebula in Hα.
3. H types are those in which the interaction takes place only in detached halos, and not in the main nebula (e.g., NGC 6853, NGC 7293).
4. The S types are thick shells. This grouping is somewhat unsatisfactory, since the two examples given this designation are very different. WDHS 1 appears as an elliptical ring, whereas IW 2 is very filamentary and appears to be a shell rather than filled because there appears to be almost no emission between the filaments. Interestingly, neither nebula reveals [O III] emission, a situation which can only be explained if the nebulae are indeed thick shells: the central zones often reveal quite strong [O III], but dilution is sufficient to reduce the flux to about 1% of Hα at the outer edge.
5. C types are those that appear crescent shaped. They are often also filamentary (see below), like S188 and DHW 5. This grouping contains the most extreme example of the PN-ISM interaction, in which the intrinsic morphology of the nebula has been destroyed by the interaction.
6. The letter f is a qualifer to the types given above, in all cases in which filaments are a dominant part of the morphology. Thus, it has been given for those like S188, but not MWP 1, in which there is some filamentary structure in one of the quadrants, but it is not a dominant feature.

8. NOTES ON THE INDIVIDUAL NEBULAE

Figures 1–15 (Plates 48–62) show images of most of the nebulae discussed here.

8.1. *Planetary Nebulae Larger than 8′*

Abell 7.—Of those planetary nebulae that do not interact with the ISM, this is the largest. There are a number of asymmetric enhancements that reveal a sharp drop in ionization, none of which appear on the perimeter of the nebula. Although these could be interaction features that happen to lie on the face of the nebula, an Hα image obtained at the KPNO 4 m by G. H. Jacoby (1995, personal communication) has convinced us that these are embedded within the nebula and are not due to the ISM. The images in Figure 10 are smoothed with a 5 × 5 box (equivalent to 10″.3 × 10″.3) for ease of presentation.

Abell 21.—This one-sided nebula, whose central star is

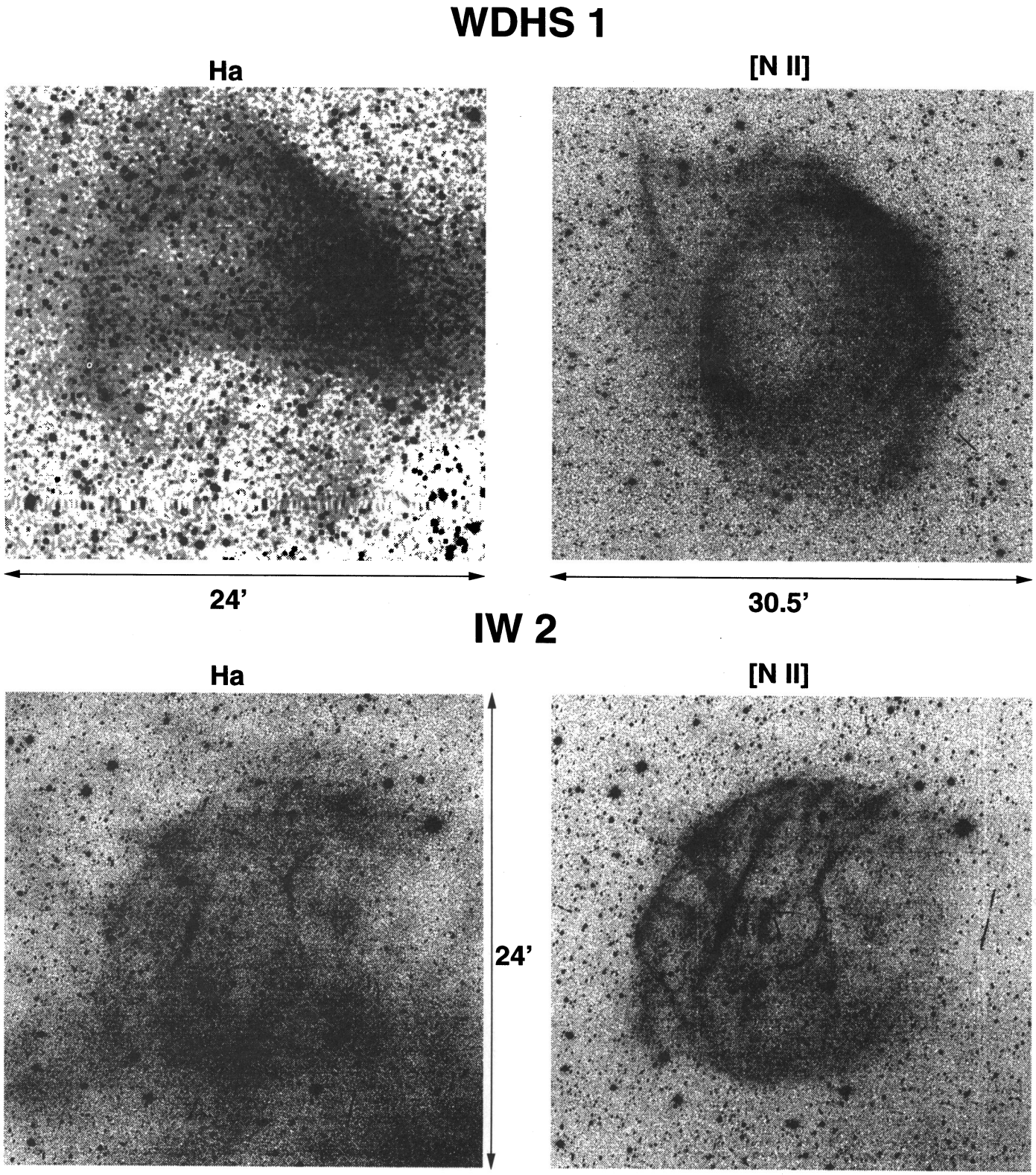

FIG. 1.—WDHS 1 and IW 2. As with all the subsequent figures, north is to the top and east is to the left. The filters used are labeled in the figures themselves. The Hα image of WDHS 1 has been smoothed with a 10 × 10 box for ease of presentation (equivalent to 20″.6 × 20″.6).

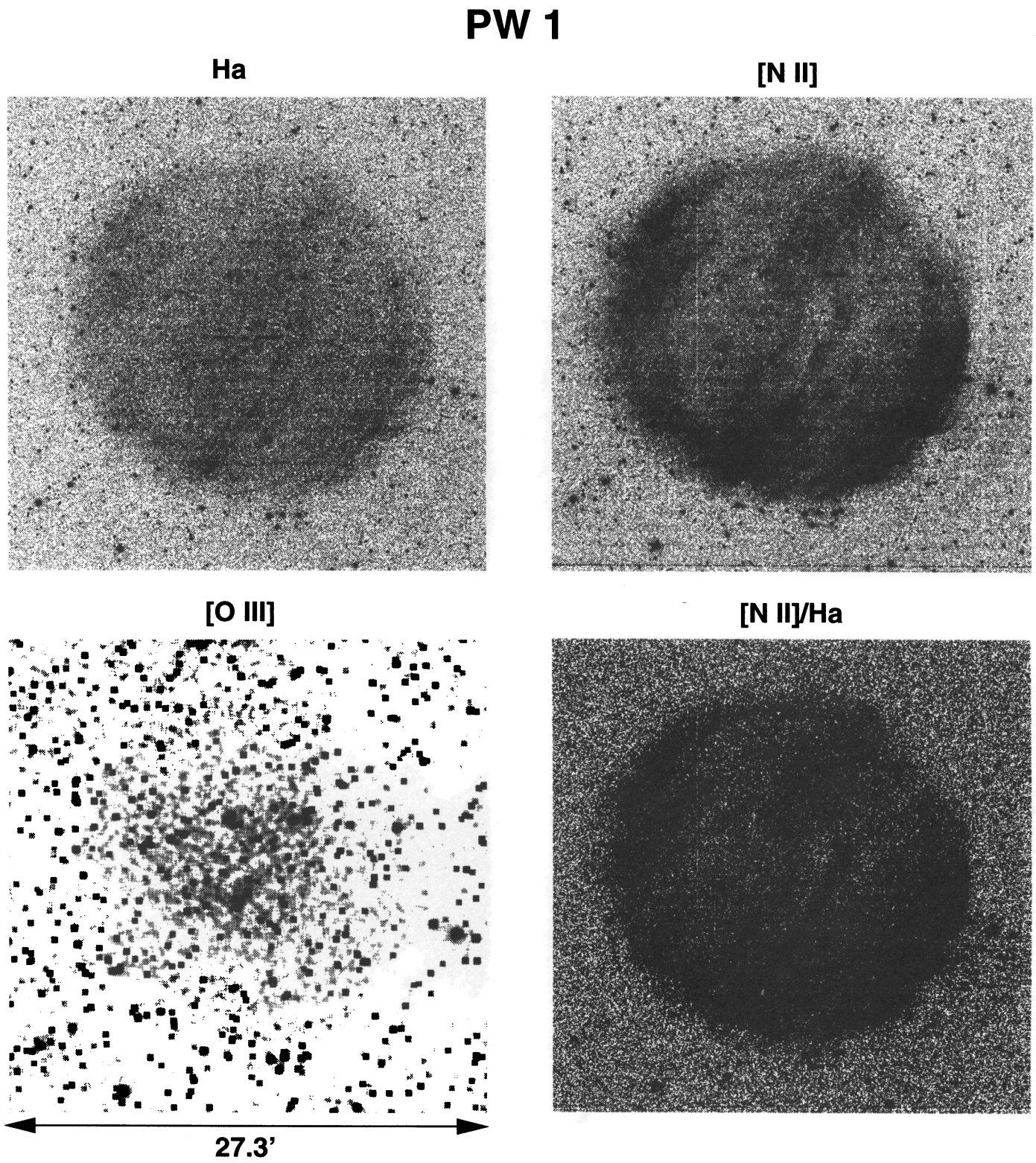

FIG. 2.—PW 1. The [O III] image has been smoothed with a 10 × 10 box (equivalent to 20″.6 × 20″.6)

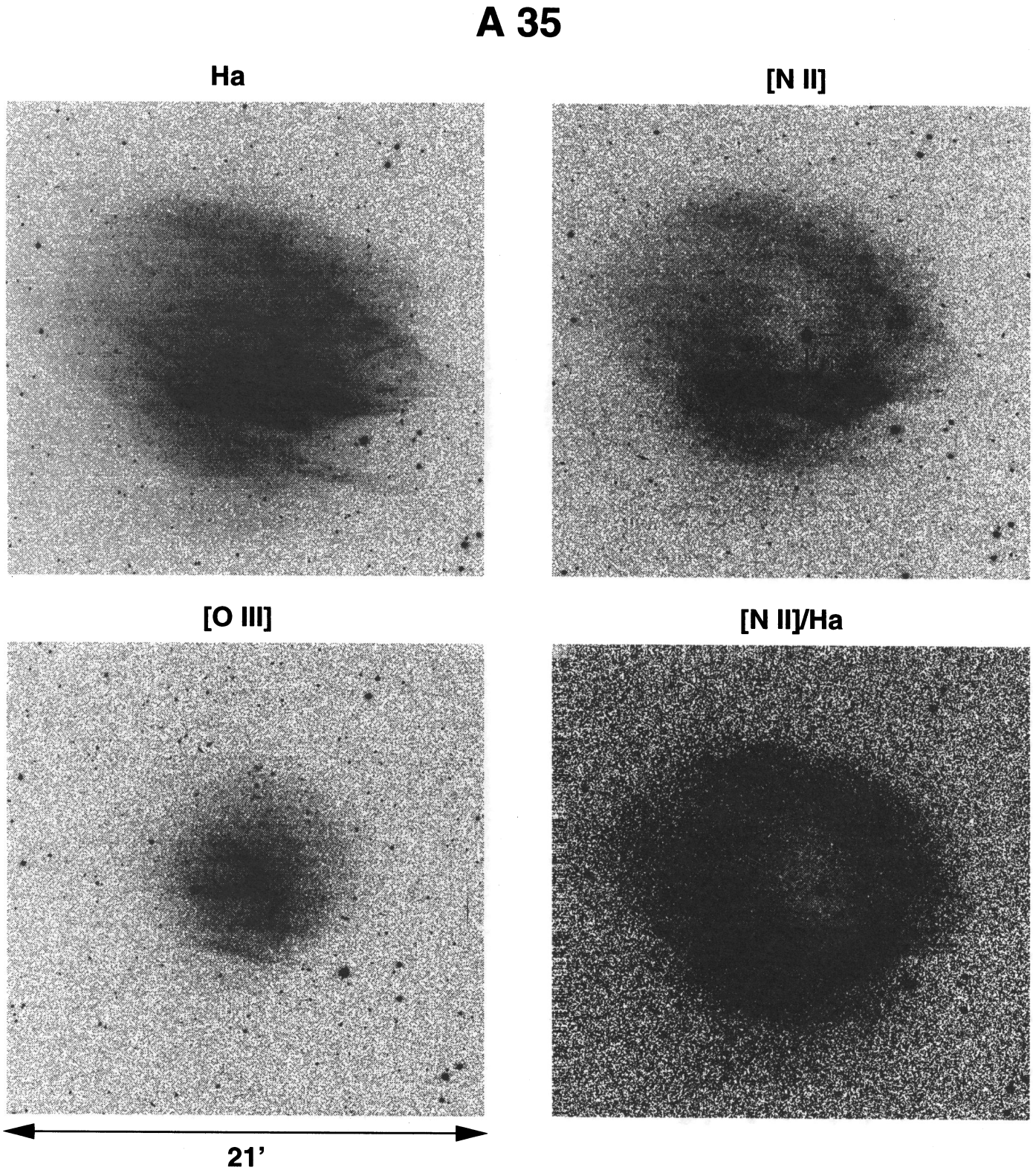

FIG. 3.—A35

Abell 74

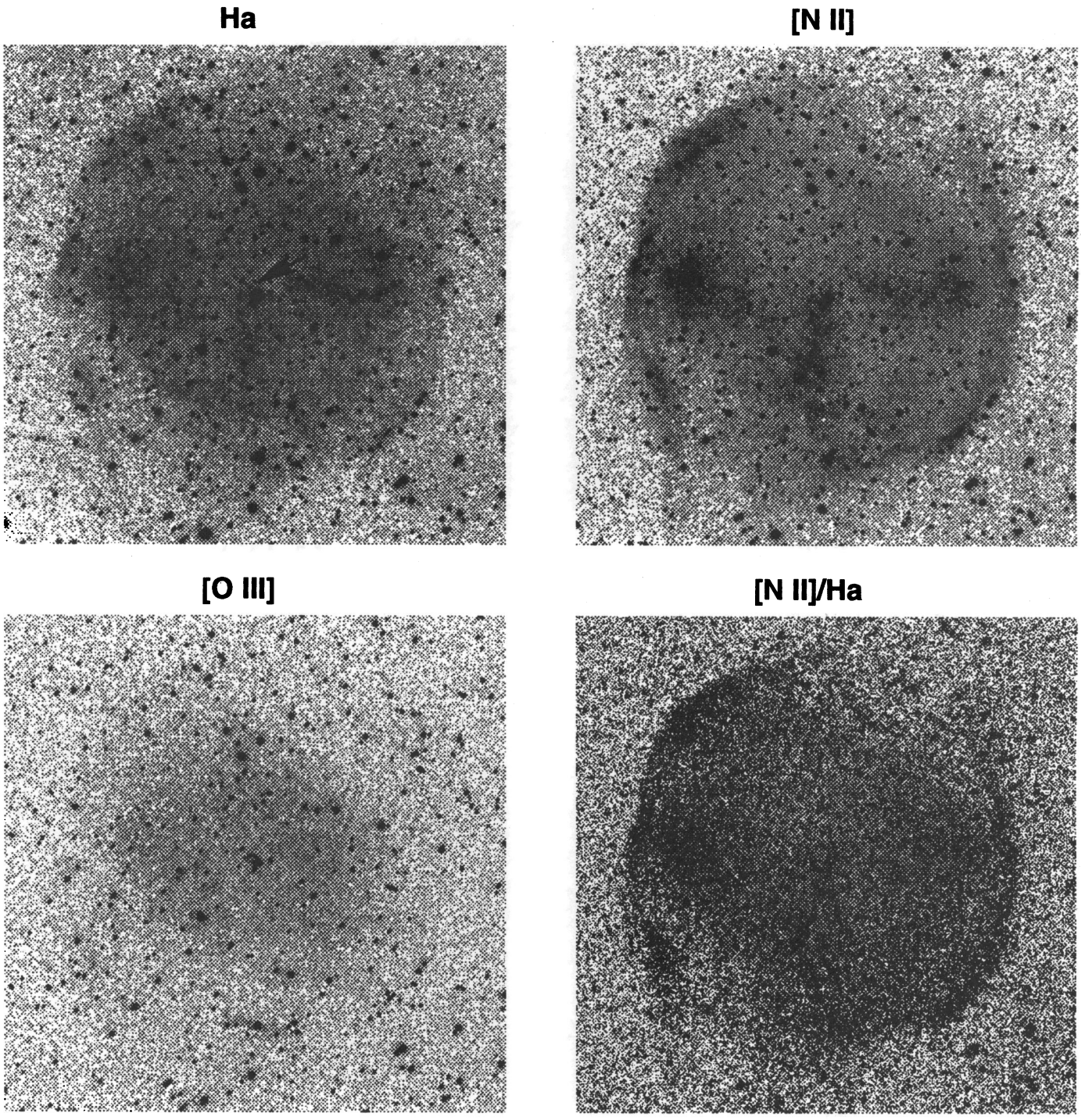

FIG. 4.—A74

TWEEDY & KWITTER (see 107, 258)

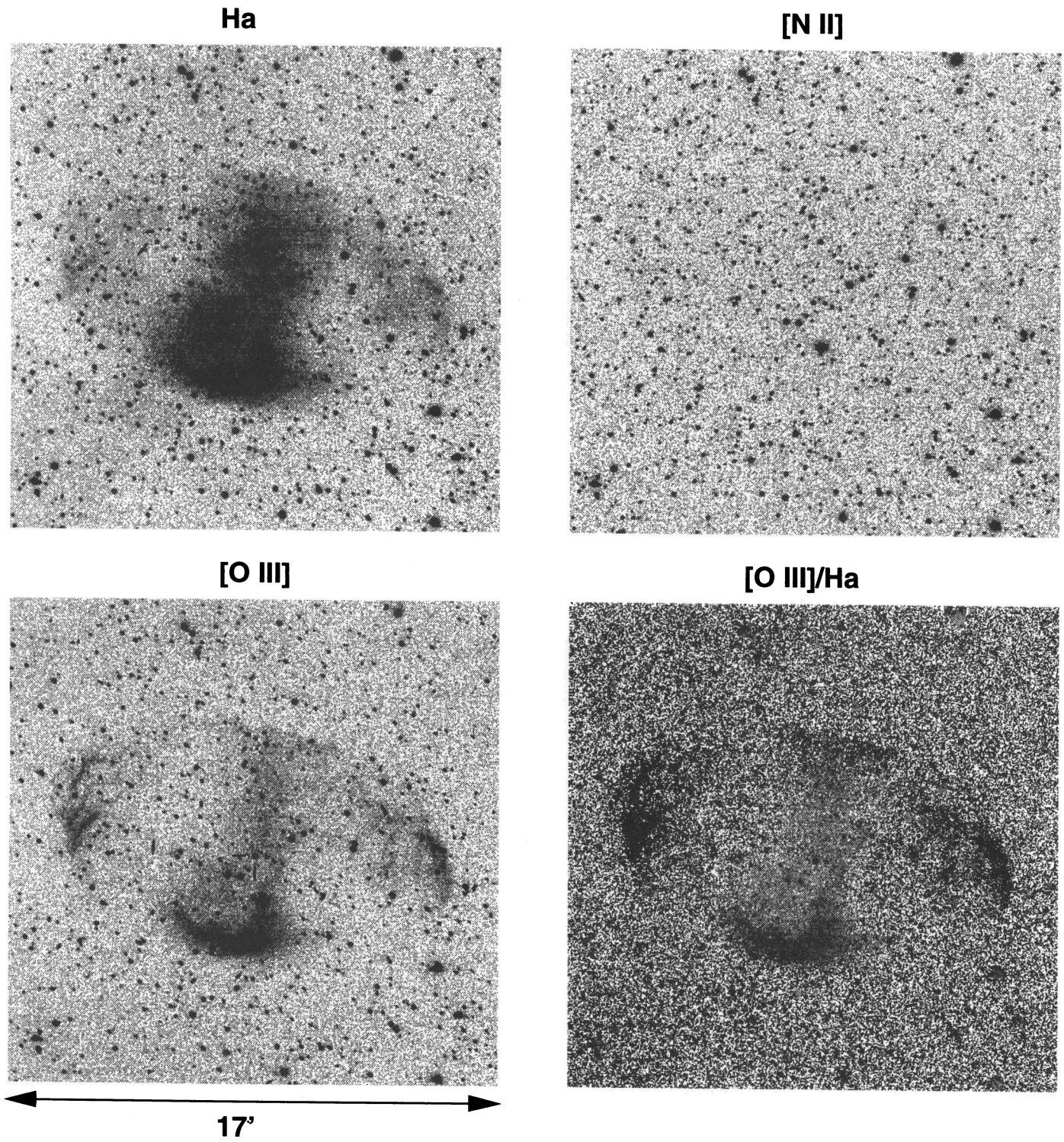

FIG. 5.—MWP 1

TWEEDY & KWITTER (see 107, 258)

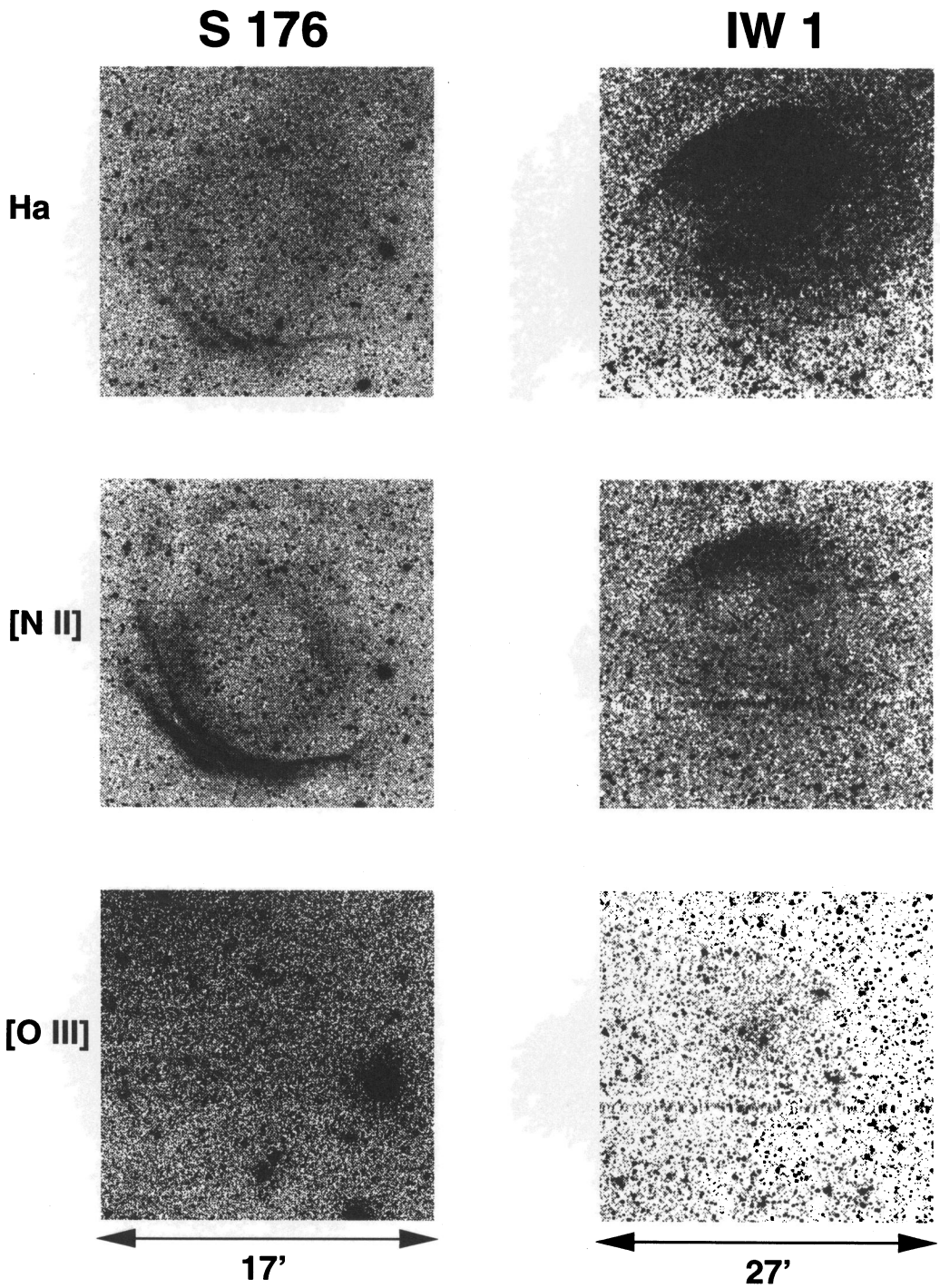

FIG. 6.—S176 and IW 1. The images of IW 1 are smoothed with a 5 × 5 box (equivalent to 10″.3 × 10″.3)

TWEEDY & KWITTER (see 107, 258)

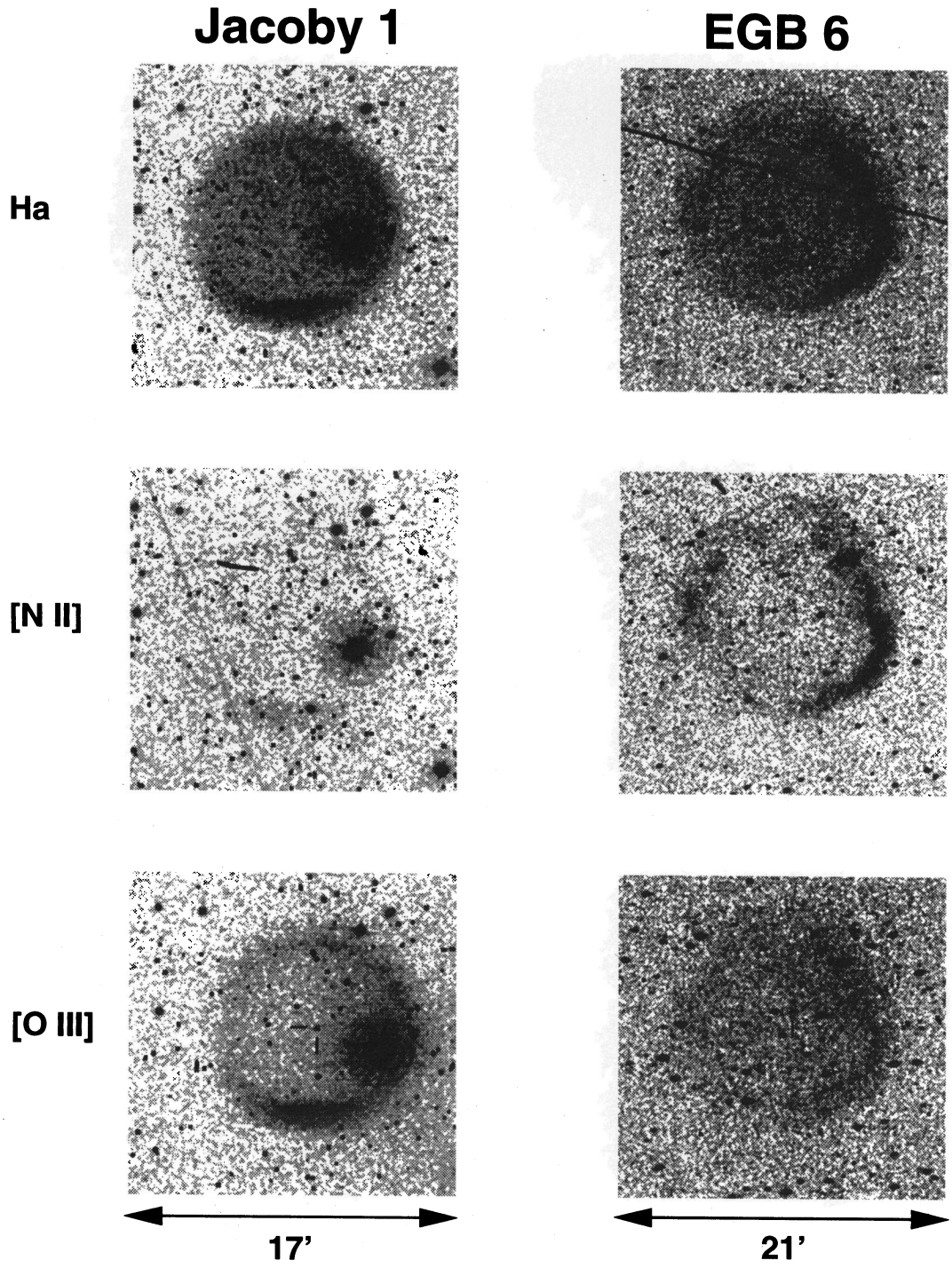

FIG. 7.—Jacoby 1 and EGB 6. All images are smoothed with a 5 × 5 box (equivalent to 10.″3 × 10.″3).

TWEEDY & KWITTER (see 107, 258)

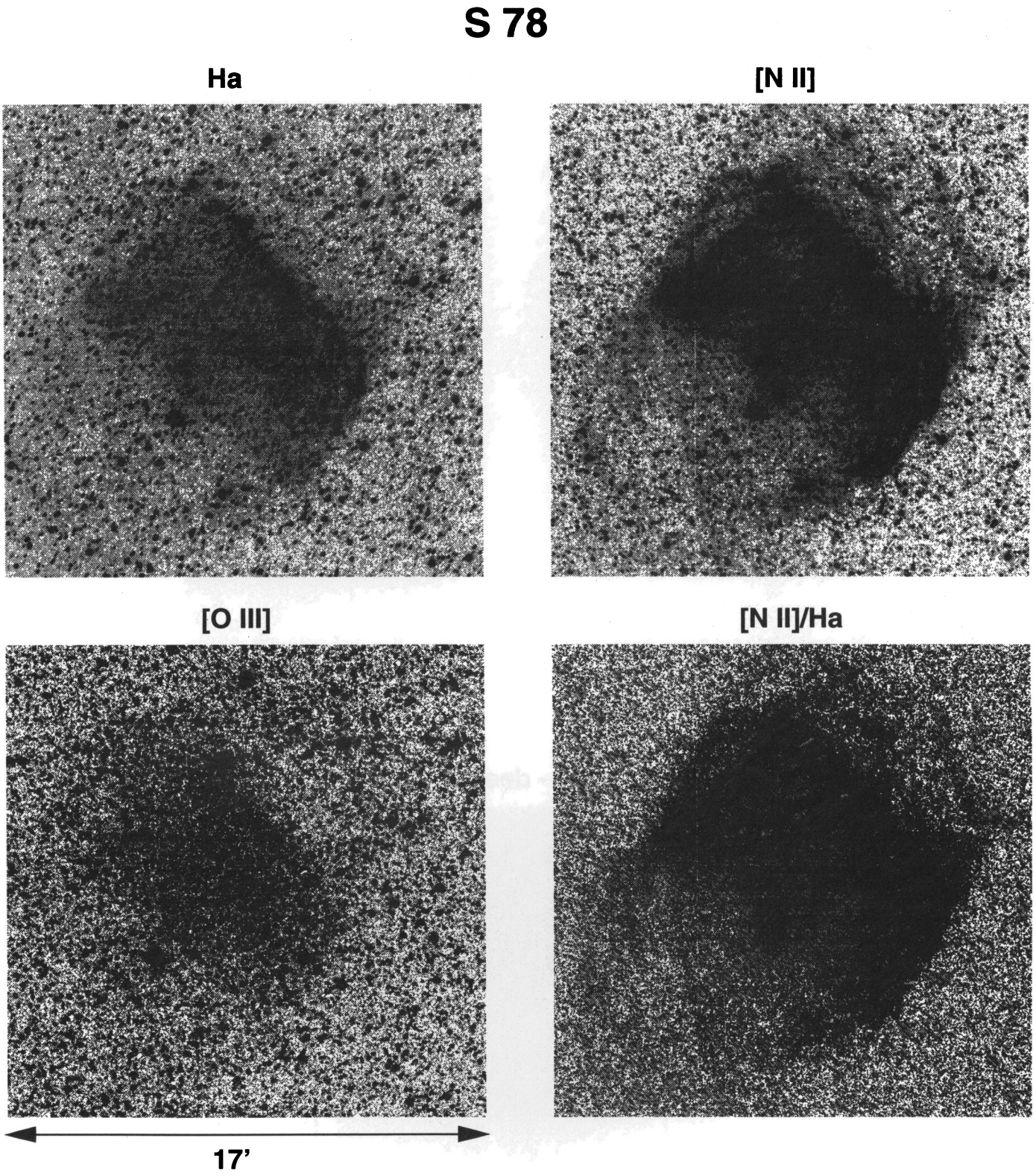

FIG. 8.—S78

TWEEDY & KWITTER (see 107, 258)

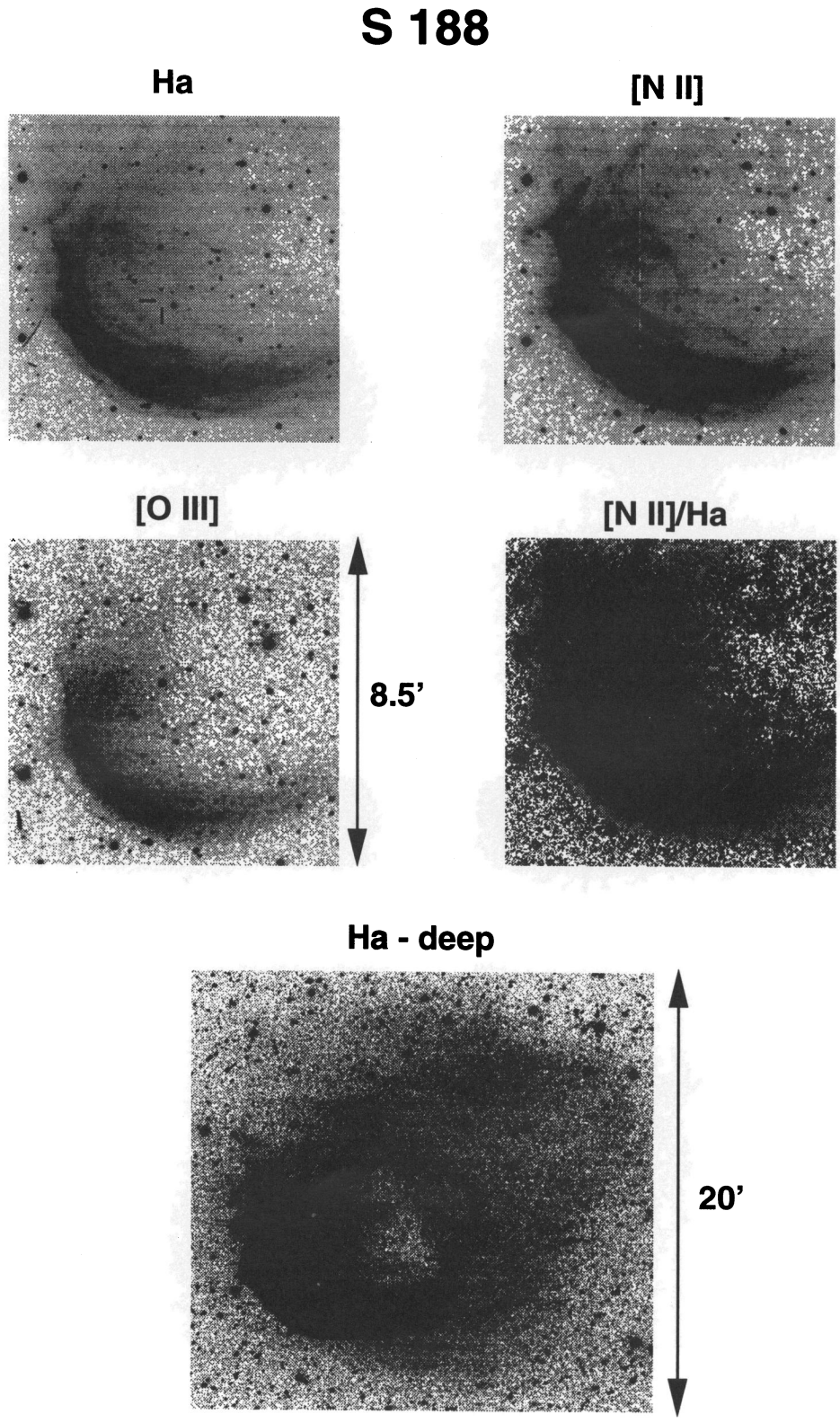

FIG. 9.—S188

TWEEDY & KWITTER (see 107, 258)

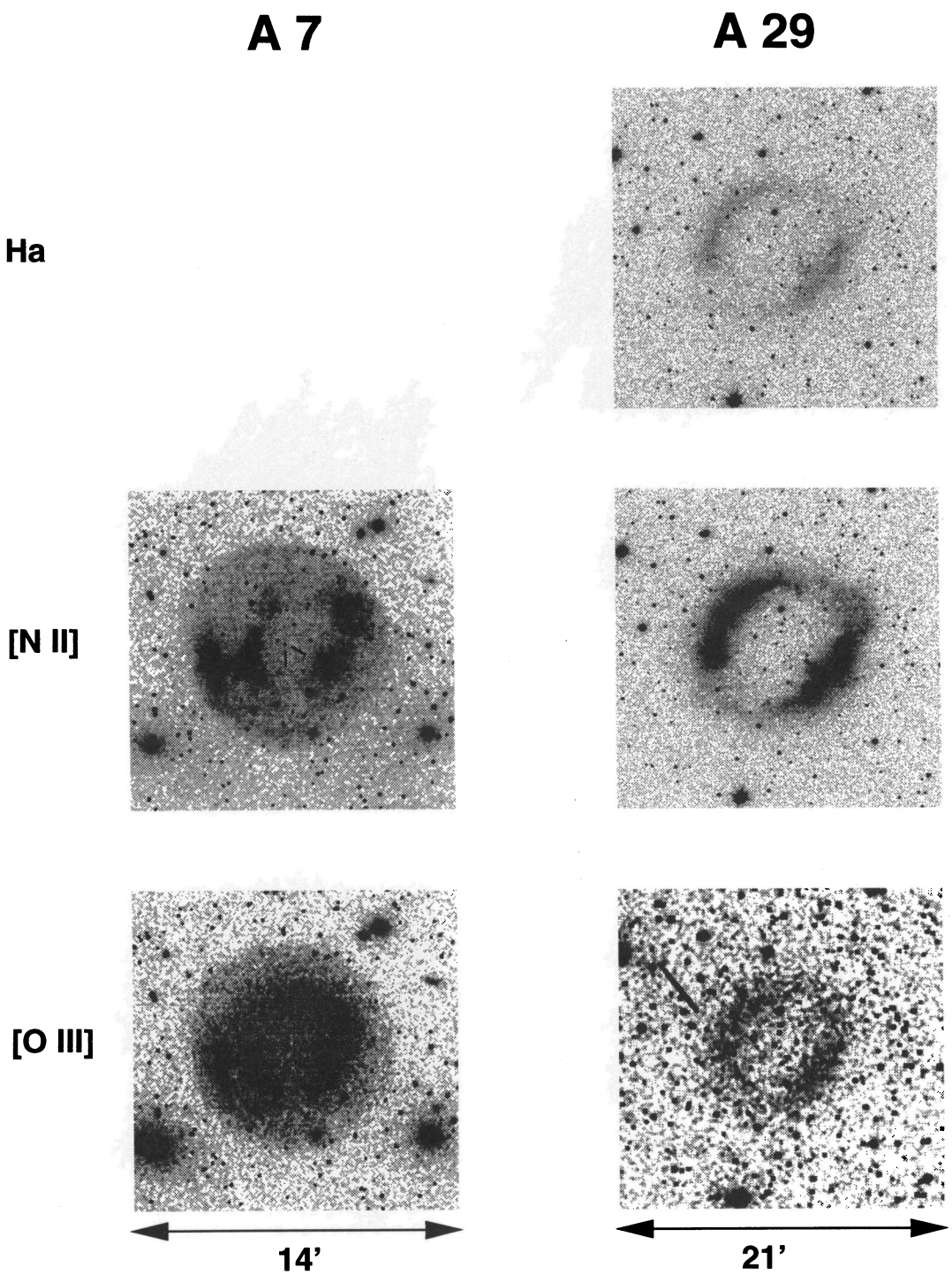

FIG. 10.—A7 and A29. Both images of Abell 7 and the [O III] image of Abell 29 are smoothed with a 5 × 5 box (equivalent to 10".3 × 10".3).

TWEEDY & KWITTER (see 107, 258)

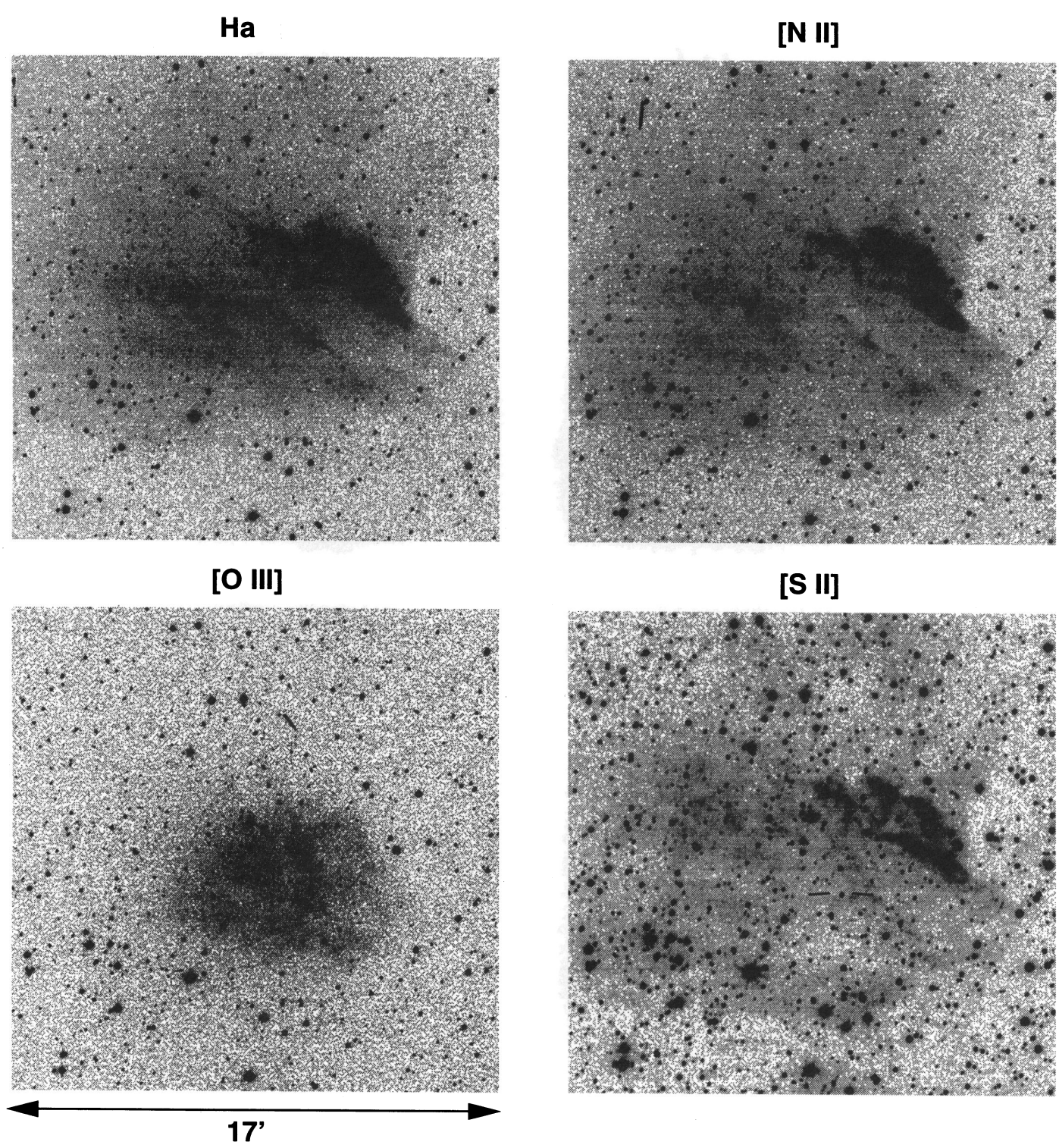

FIG. 11.—DHW 5

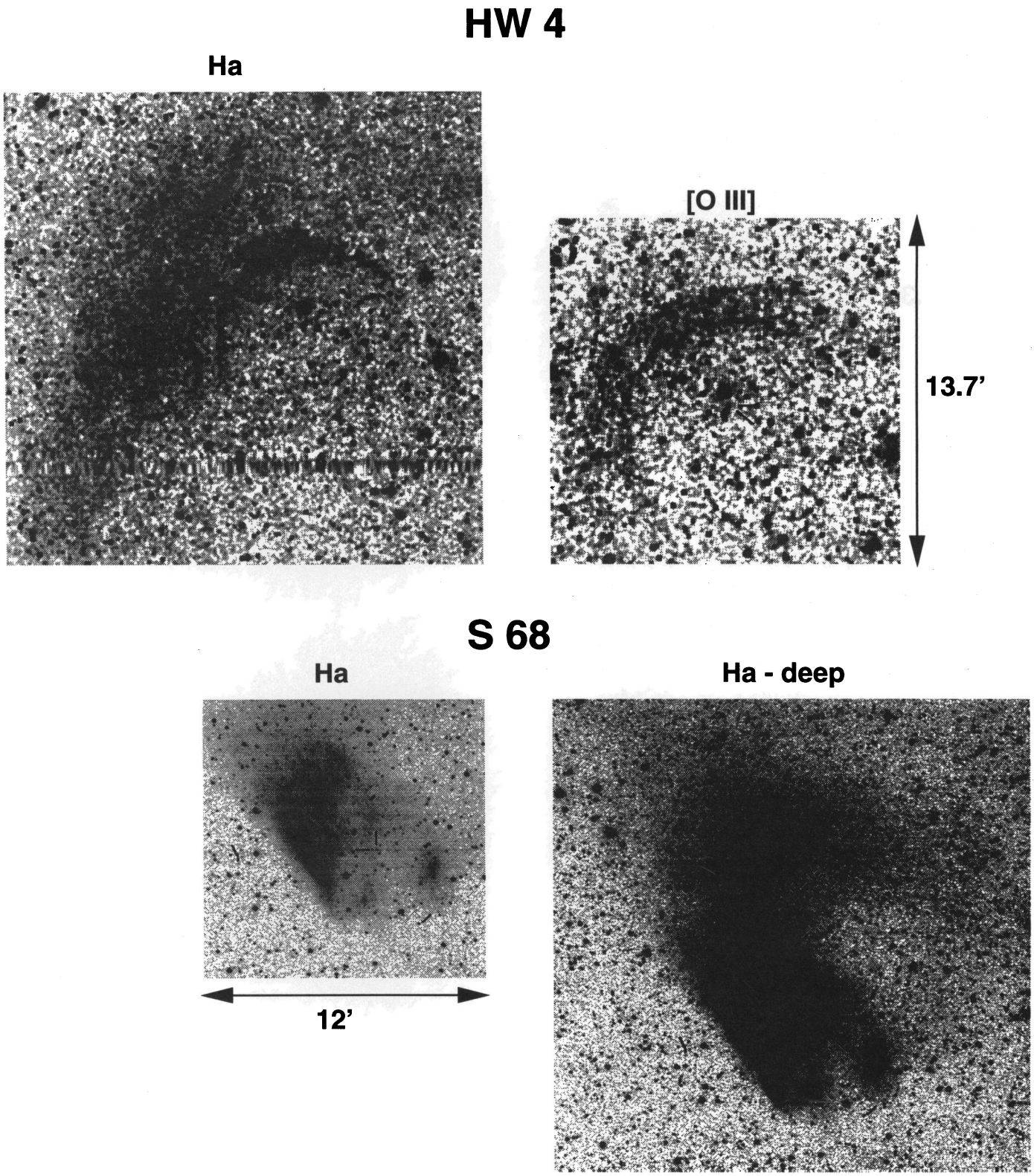

FIG. 12.—HW 4 and S68. The images of HW 4 are smoothed with a 5 × 5 box (equivalent to 10″.3 × 10″.3).

TWEEDY & KWITTER (see 107, 258)

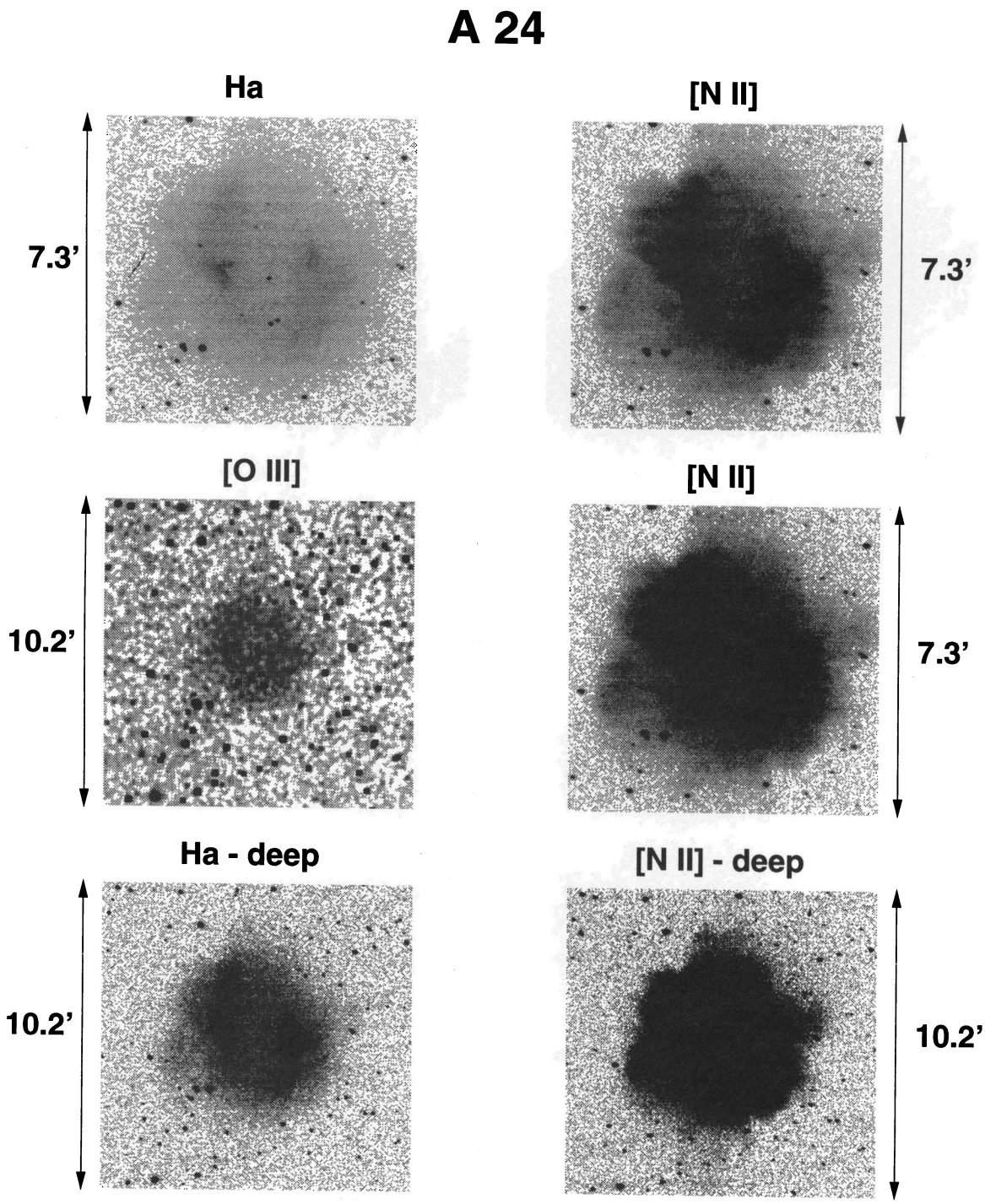

FIG. 13.—A24

TWEEDY & KWITTER (see 107, 258)

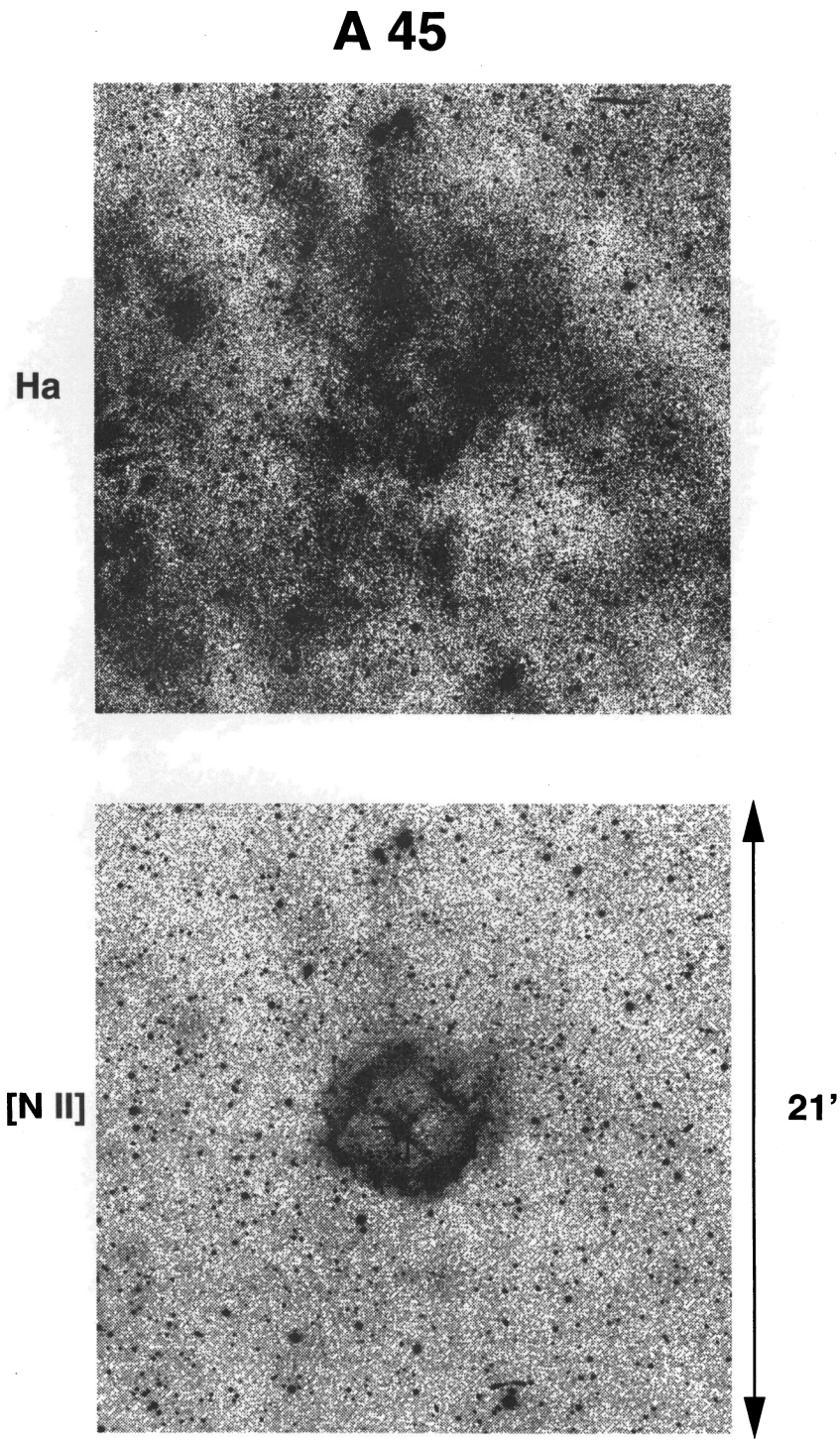

FIG. 14.—A45

TWEEDY & KWITTER (see 107, 258)

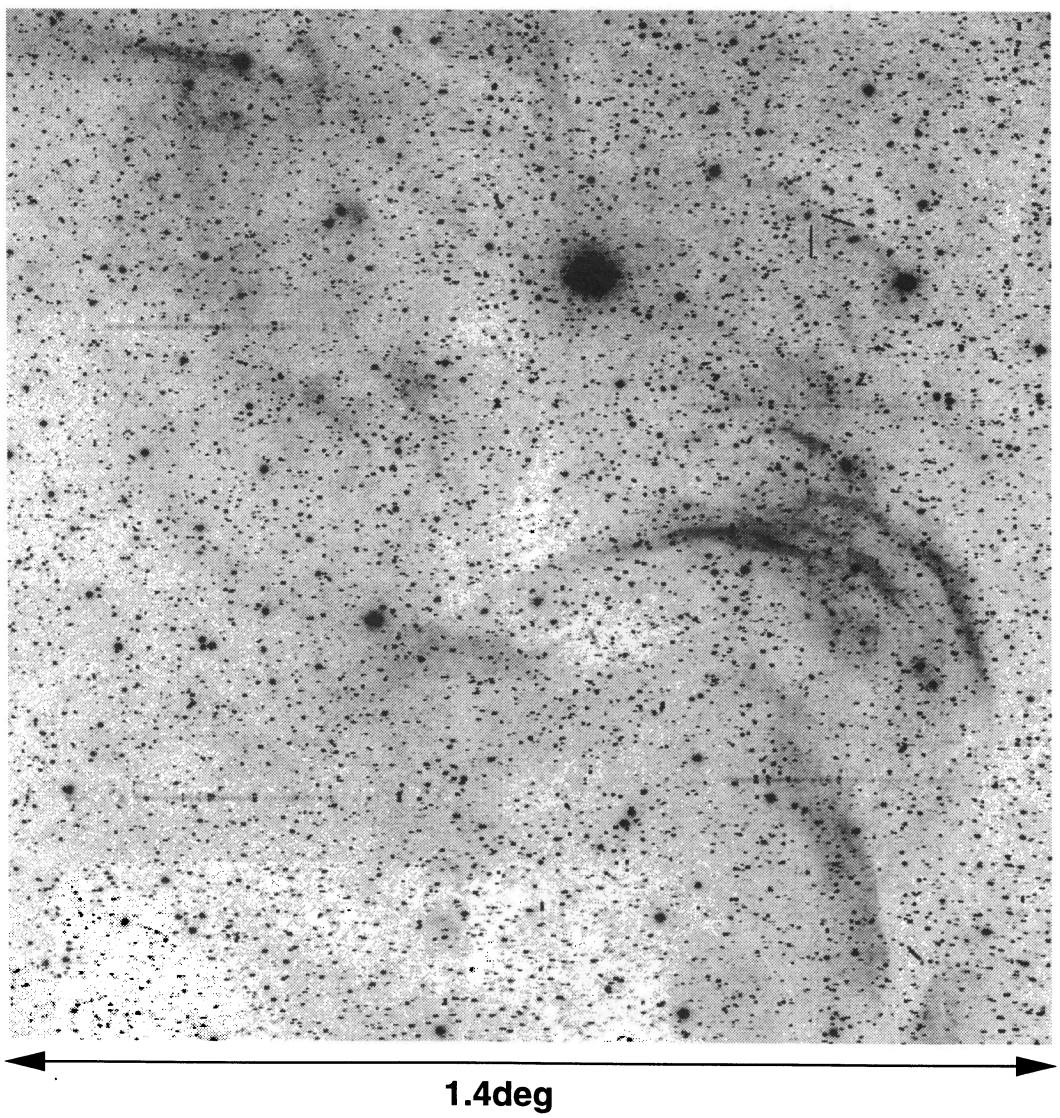

FIG. 15.—Field around BD +28 4211 (indicated) in Ha

clearly displaced from the center, is an excellent example of a PN interacting with the ISM. The Hα image displayed here reveals both a faint rim to the northwest, which completes the elliptical perimeter, and fainter diffuse material downstream. An [O III] image was published in Kwitter, Jacoby, & Lawrie (1983). We discuss this phenomenon in greater detail for the similar S188.

Abell 29.—Like Abell 7, this nebula contains some significant asymmetry and also reveals a high [N II]/Hα. Its perimeter is diffuse and does not reveal a distinct edge anywhere. We infer that this nebula is also not interacting with the ISM. The [O III] image in Figure 10 has been smoothed with a 5 × 5 pixel box (equivalent to 10".3 × 10".3).

Abell 31.—The ionization structure, with the O^{++} Strömgren zone restricted to a small region close to the central star, is typical of many ancient nebulae. However, the interior is unusual in having a convoluted morphology. The southern rim is bounded by a wide bow shock, where the interaction is taking place, while the northern side is diffuse (Tweedy & Kwitter 1994a).

Abell 35.—Abell 35 has had a controversial history of interpretation, despite being one of the first nebulae regarded as interacting with the ISM, and it remains a somewhat perplexing object. At the center of the [O III] image is a bow shock centered on a G star (Jacoby 1981). Jacoby suggested that this star is a binary, with a degenerate companion that is the central star of the nebula. Subsequent *IUE* observations confirmed this (Grewing & Bianchi 1988) and also revealed Mg II emission lines, which could indicate that it is a cataclysmic or precataclysmic binary. However, Jasniewicz, Lapierre, & Monier (1994) showed that the G star is a rapid rotator, which is thus likely to be responsible for the emission lines. The bow shock is embedded in a much larger cloud, which Hollis et al. (1996) believe to be an ambient interstellar cloud, through which the mass-losing Abell 35 system is plowing. However, a yet more curious feature is the two parallel structures to the south of the nebula, which are prominent in [N II] and Hα. Hollis et al. believe that this may be a tunnel carved by a star passing through long before the arrival of the Abell 35 system. Quite why all this excitement should be occurring in this one place remains to be explained, but it serves to cast some doubt on whether all of the visible nebulosity is actually planetary nebula. For ISM studies, it will continue to be of considerable interest, particularly when it is more fully understood (Fig. 3).

Abell 36.—This is a point-symmetric nebula which shows no sign of an interaction with the ISM.

Abell 74.—Significant asymmetric enhancements exist on the edge and are accompanied by an increase in the [N II]/Hα, characteristic signs of an interaction with the ISM. Similar patches appear on the face of the nebula; the only difference is probably in the viewing angle. There is a significant amount of symmetry associated with these patches, although other parts, particularly on the perimeter, are notably lacking in symmetry. As with Abell 31, the [O III] zone is small (Fig. 4).

DHW 5.—This is a predominantly one-sided nebula, with marked filamentary structure dominating the morphology. Note the large amount of diffuse material surrounding the bright filaments, which could be interstellar material being ionized by the central star. The POSS plates show that the region is fairly dusty. Extensive filamentary material exists to the south, possibly from a nearby supernova remnant (Fig. 11).

EGB 6.—Unlike its central star (Liebert et al. 1989), the nebula is normal and easy to understand. The eastern half is fairly spherical, while the western half is somewhat distorted and has a strong enhancement on the edge, which is the brightest part of the nebula in all three observed lines (even [O III]). We conclude that this PN is definitely interacting with the ISM (Fig. 7).

HFG 1.—This nebula was discovered on the Milky Way Emission-Line Survey by Heckathorn, Fesen, & Gull (1982) and has a bright enhancement at the southeast rim, which is indicative of an ISM interaction.

HW 4.—There is one prominent arc, and a second feature slightly to the north-northeast that may be a weaker filament. This one-sided structure appears to be typical of planetary nebulae in advanced stages of their interaction with the ISM. There is considerable weak diffuse Hα in close proximity to the nebula, most notably a strip to the east, running southeast to northwest. Our colleague, D. Maraziti, remarked that this nebula resembles a coffee-mug stain, and, indeed, that is probably the most accurate and concise description of it (Fig. 12)!

IW 1.—This is an exceptionally faint nebula, revealing little detail. There is a steady increase in brightness from the diffuse southwest sector to a fairly bright, sharp-edged enhancement to the north-northeast. Some faint filamentary structure may exist in the center and to the south. The overall appearance is consistent with the nebula being in an advanced stage of the PN-ISM interaction (Fig. 6).

IW 2.—In Hα, IW 2 is barely distinguishable from the relatively bright diffuse interstellar emission. However, in [N II] it stands out quite prominently and is particularly distinguishable by the several bright, fairly parallel filaments. It appears to be an obvious precursor to classic one-sided nebulae like Abell 21. The interstellar emission may just be in the line of sight, and not in the same locality, since the regions of strongest interaction coincide with areas with weak diffuse Hα (Fig. 1).

Jacoby 1.—This nebula was recently discovered by Jacoby & van de Steene (1995). It is very circular, with a general enhancement toward the rim that is particularly marked in a patch to the south. Both characteristics indicate an interaction with the ISM. The central star, PG 1520+525, is extremely hot and has exotic abundances, bein devoid of H and rich in He, C, and O (Werner, Heber, & Hunger 1991) (Fig. 7).

LT 5.—Like A36, LT 5 is a point-symmetric nebula and shows no sign of an interaction with the ISM (Longmore & Tritton 1980).

MWP 1.—MWP 1 is the only nebula in our sample that is both definitely bipolar and also interacting with the ISM (Appleton, Kawaler, & Eiffler 1994; see also comments on WDHS 1). It is therefore particularly instructive in understanding the relative roles of intrinsic structure and the ISM. Clearly, the bipolarity is intrinsic to the nebula (which could be due to a close binary central star or one that has a significant magnetic field; e.g., Livio 1993); but there are strong asymmetries in addition to that. This is particularly true of the central bar, whose southern end has a strong, sharp enhancement, while the northern end is quite diffuse. It seems quite likely that the other two lobes are also interacting with the ISM; and indeed the easternmost one shows some filamentary structure. But it is the enhancement in the bar that is the most convincing evidence for the PN-ISM

interaction. The central star, RX J2117.1+3412, was discovered in the *ROSAT* XRT survey and is similar in composition to PG 1520+525, except that it is even hotter and is also a pulsating GW Vir star (Fig. 5).

NGC 6853, NGC 7293.—Both these objects will be discussed extensively elsewhere (e.g., Kwitter, Downes, & Chu 1996). In neither case does the main shell show signs of interaction with the ISM, while both do show asymmetric haloes. The situation is rather clearer in the case of NGC 7293, since the halo appears to have been ejected symmetrically, with the northeast half appearing to have run into a higher density region than its southwest counterpart. We argue by extension that this is also true for the halo of NGC 6853, although the southern half of the halo is currently undetected.

PW 1.—Its spherical appearance on the POSS is misleading: the images presented here show strong evidence of an early stage in the PN-ISM interaction. Much of the rim is enhanced, with the exception of the northern sector, and there is strong filamentary structure already developing, running south-southeast–north-northwest. Current evidence indicates that its central star is remarkably cool (Napiwotzki 1993), although an analysis of the higher-order Balmer lines (such as Hδ) still has to be done (Fig. 2).

RE 1738+665.—Two concentric filaments were found close to this hot white dwarf (Tweedy & Kwitter 1994b).

Sharpless 78.—This nebula is distinguished by a markedly filamentary appearance in [N II], which is less apparent at Hα. Deeper reproductions of the [N II] image show clearly that the major and minor axes are switched, an effect which is just apparent in Figure 8.

Sharpless 174.—This cleft hoof-shaped nebula has a unique morphology and appears to be interacting with the ISM on the eastern edge. The central star is of very low mass (consistent with 0.3 $M_{\odot}$) (Tweedy & Napiwotzki 1994), which is consistent with the prediction that it may be part of a double-degenerate system (Marsh, Dhillon, & Duck 1995). (Contrary to the comments of Tweedy & Napiwotzki, it is the sharp edge and displaced central star that indicate an interaction with the ISM is taking place, not the ionization stratification.)

Sharpless 176.—This nebula has a somewhat surprising morphology insofar as there appears to be two detached components: a central filled sphere, and two long filaments to the east which are not obviously connected to the rest of the nebula (Fig. 6).

Sharpless 188.—This has the highest surface brightness of the ancient planetary nebulae and is dominated by a very one-sided filamentary structure. The deeper reproduction of the Hα image in Figure 9 shows much faint, rather homogeneous material from the opposite side of the bright filaments to the northwest. The Hα surface brightness in the tail is a factor of $\approx$30 below that of the bright filaments. Although it has the appearance of a comet tail, a simpler explanation for the faint material is that it is just the northwest side of the nebula that has diffused away. This may imply a highly inhomogeneous ISM in the vicinity of S188: one that produces the bright filaments to the southeast but is essentially absent to the northwest. Note also the central cavity, which would be more difficult to explain if the tail had a comet-like origin. There is also a moderately faint filament which appears to define an ellipse with the bright filaments (Fig. 9).

Sharpless 216.—This is the closest known planetary nebula, which has been discussed extensively in Tweedy et al. (1995).

Ton 320.—As with RE 1738+665, two concentric filaments were found close to this hot white dwarf (Tweedy & Kwitter 1994b).

WHDS 1.—This nebula has a substantially different appearance in [N II] compared to Hα; indeed, while the [N II] reveals an elliptical ring with a fish tail to one side, the Hα image prompted Liebert, Bergeron, & Tweedy (1994) to regard the nebula as bipolar. This discrepancy may be explained by the fact that the apparent bar in WDHS 1 extends beyond the elliptical ring and may be an interstellar feature. Such a line-of-sight coincidence would be unfortunate but would explain why the bar does not appear in either [N II] or [O III] (Fig. 1).

8.2. *Three Smaller Nebulae*

Abell 24.—This nebula is unusual in having a very high [N II]/Hα ratio ($\approx$4.3 in the brightest regions), but its perimeter is diffuse all around. It cannot therefore be interacting with the ISM. Note also that the nebula appears to be somewhat point symmetric (Fig. 13).

Abell 45.—In Hα, this nebula can barely be distinguished from its surroundings, which are of a similar surface brightness. However, the [N II] emission in the region comes from the nebula alone. Note that the perimeter is distorted particularly in those directions in which the ISM is brightest, which suggests that the nebula is indeed interacting with the same interstellar material that is visible (Fig. 14).

Sharpless 68.—The central star is neither very central nor displaced in the direction of the greatest ISM interaction. Clearly, the surrounding ISM is highly inhomogeneous: the eastern edge is both quite sharp and unusually straight, whereas elsewhere the edge is quite diffuse. There is faint material to the north and east of the PN, and it is unclear whether this is from the nebula, or ISM illuminated by the central star (Fig. 12).

9. PROBING THE ISM: A NAÏVE ESTIMATE FOR THE FILLING FACTOR OF CORONAL GAS

The filling factor of coronal gas (f) has long been a controversial topic within studies of the interstellar medium. In a recent review of this phase of the ISM, Spitzer (1990) summarized recent estimates, which varied between 0.1 and 0.9, and concluded that "... (the) observational results are about as inconclusive as the theoretical ones." Since then, some degree of consensus is being achieved, insofar as the models of both Slavin & Cox (1993) and Ferrière (1995) suggest low values of f in the disk ($<$18% and $\approx$30%, respectively). The observational data are somewhat ambiguous and are often strongly model dependent(!). For example, Higdon & Lingenfelter (1980) derived a high value $f \approx 0.9$, but they used a method that relied on understanding the evolution of the surface brightness. McKee (1987) also argued for a high value, with $0.4 < f < 0.7$. In addition to the O VI data that will be discussed below, the two key reasons were the survival of dust grains in the warm phase of the ISM and the acceleration of cosmic rays. Both lines of reasoning have their problems. As was recognized by McKee et al. (1987), dust grain survival is enhanced significantly by the inclusion of a realistic magnetic field. Arguments based on cosmic-ray acceleration rely also on models of the development of SNR shocks. Probably the most direct method is the analysis of the lines of sight to hot stars.

Originally performed by Jenkins (1978), this was redone by Shelton & Cox (1994), but even their results are dependent upon the assumed origin of the O VI: a superbubble interpretation leads to $0.08 < f < 0.25$, while presuming the ion to originate in regions of cloud evaporation leads to $0.008 < f < 0.025$. Furthermore, since this is a line-of-sight analysis, the actual distances to the clouds are unknown.

Ancient planetary nebulae can potentially be very effective probes of the filling factor of coronal gas both because they are at known locations, and because they are distributed uniformly throughout the galaxy. To do this properly requires the density of the surrounding gas to be determined, for which reliable magnetohydrodynamic (MHD) models need to be computed. However, a naïve estimate may be obtained much more simply. The sound speed in gas is given by $c_s^2 = \gamma kT/\mu$, where k, T, and c_s have their usual meanings and μ is the mean molecular weight of the gas. In warm ionized gas, with $T \sim 10^4$ K, $c_s \sim 10$ km s^{-1}; in coronal gas, with $T \sim 10^6$ K, $c_s \sim 100$ km s^{-1}. Since most planetary nebulae have space velocities $\sim$ a few $\times$ 10 km s^{-1}, we may infer that a shock between the PN and the ISM can form only when the nebula is moving through the warm phase, but not in the coronal phase. Therefore, we can simply count up the fraction of large planetary nebulae that are not interacting, and use that as a naïve value for the filling factor, f. This procedure is in the same spirit as a recent estimate of the filling factor of dust-bearing gas by Gaustad & van Buren (1993). In both cases, the major strength of the procedure is the directness and simplicity.

From Table 3, we find that four out of the total sample of 27 are not interacting, which by itself would imply $f \approx 0.15$. However, the miserable sample size means that there is a very large error ($\sim$20%). Furthermore, those that are interacting are easier to detect than those that are not, so that faint, uniform surface brightness nebulae in coronal gas are more likely to be overlooked; this effect would suggest that f has been underestimated. This is particularly clear in the cases of the newly discovered nebulae around Ton 320 and RE 1738+665, which are extremely faint, and would not have been detected if they were located in coronal gas. Several groups have scoured the PSS plates for faint nebulae, so it is probably meaningful to include only those that were discovered on the PSS; this therefore excludes LT 5, Jacoby 1, and MWP 1, which all have high [O III] and no [N II]. Several of those remaining were reported originally as having uniform surface brightness, but they are now known to be interacting (e.g., PW 1, Purgathofer & Weinberger 1980; IW 1 and 2, Ishida & Weinberger 1987), so that there is some justification for presuming that this criterion leads to a fairly homogeneous sample. Countering this selection effect, though, is the presumption that all those that are noninteracting would interact if they were placed in the warm ISM; this is probably a gross oversimplification, as implied by the fact that three of the four that are noninteracting are among the six smallest in the list; this suggests that f has been overestimated. Combining the initial estimate, together with the large error, and presuming that the other two effects roughly cancel, leads to a naïve value of $f < 0.4$.

The main benefit of this exercise is to demonstrate the feasibility of using ancient planetary nebulae to derive a filling factor of coronal gas. Clearly, a serious estimate requires that a large sample of objects ($\approx$100) be obtained, together with a detailed knowledge of distances and space velocities. Another key issue is to determine the density profile of the medium surrounding those planetaries that are interacting: for example, the interaction regions of Abell 74 are very patchy. Nevertheless, a real and present benefit of the current estimate is that it does argue strongly against the highest estimates of the filling factor.

10. AMBIENT INTERSTELLAR MATERIAL

Several of the PN fields observed also revealed emission from the ISM. The importance of this is twofold: first, if the nebula is shown to be interacting with interstellar material that is also visible, this would be particularly valuable for studying the PN-ISM interaction; second, whether or not this is the case, this shows that the ISM can be studied with direct imaging, even leading to the study of its morphology.

10.1. *Is the Visible ISM a Line-of-Sight Coincidence?*

The field containing IW 2 is an excellent case study. Although some filamentary structures are prominent, the planetary nebula is ill defined in Hα because it appears to merge smoothly with the ISM. However, while the nebula is rather brighter in [N II], no emission from the ISM is evident. While velocity information would be desirable for discerning whether it is the visible ISM with which the nebula is interacting, there is other, more circumstantial evidence that the two are a line-of-sight coincidence. First, if the two were interacting, the interstellar material would be expected to lie predominantly around the regions in which there is a shock in the PN, whereas in reality there is no such correlation. Second, the visual appearance of the nebula together with the absence of any detected [O III] emission suggests that it is essentially a filamentary thin shell: since the low surface brightness implies a low electron density, any visible ISM located just outside the nebula would show a similar [N II]/Hα ratio.

Abell 45 is a much smaller (and more distant) PN, where the PN in Hα is completely indistinguishable from the surrounding ISM. There is considerable ignorance about the central star; only its possible identity is known (Kwitter, Jacoby, & Lydon 1988). However, in this case it is noteworthy that the ISM is most prominent in Hα precisely where in [N II] it appears most disrupted. Therefore, this is a much better candidate for supposing the PN to be interacting with the visible ISM.

10.2. *The Waddling, Quacking, Non-Duck*

Finally, we show in Figure 15 the 1°.4 field close to the hot white dwarf standard star BD +28 4211, in order to record that the filamentary arcs to the south do not belong to its planetary nebula. The appearance of these arcs is highly reminiscent of an ancient PN (see, for example, Tweedy & Kwitter 1994b). The star itself, with $T \approx 85{,}000$ K (Napiwotzki & Schönberner 1993), has many of the characteristics expected of an old central star but is located outside the circumference of the nebula. If it were responsible for the nebula, it must therefore have moved outside it, and it should have a proper motion away from the center of the nebula, i.e., toward the north. However, Hall (1953) measured it and found it to be traveling more or less in the opposite direction—it is moving toward the nebula. We were so surprised when we read this that we asked J. MacConnell for verification; he remeasured the proper motion using the PSS and the *Hubble Space Telescope* Guide Star Catalogue and confirmed Hall's result (J. MacConnell 1994,

personal communication). The nebulosity has also been detected in [N II], but the low ionization level is consistent with ionization from diffuse starlight: this suggests that the proximity of star and nebular arcs is a line-of-sight coincidence. Although we mentioned this result in passing in Tweedy & Kwitter (1994b), one of our colleagues rediscovered this nebulosity recently and has therefore persuaded us to bring it to wider notice.

We have benefited greatly from conversations with several people. In particular, John Mathis alerted us to the importance of sound speeds, and Harriet Dinerstein challenged us not to get carried away by our results. We are grateful to an anonymous referee for numerous comments that have led to the improvement of this paper. K. B. K. acknowledges support from a Cottrell College Science grant of Research Corporation and from the Division III Funding Committee of Williams College. Finally, we must thank Galileo and Copernicus, K. B. K.'s two rats, for not eating this paper before it was submitted.

REFERENCES

Appleton, P. N., Kawaler, S. D., & Eitter, J. J. 1994, AJ, 106, 1973
Balick, B. 1987, AJ, 94, 671
Balick, B., Rugers, M., Terzian, Y., & Chengalur, J. N. 1993, ApJ, 411, 778
Blöcker, T., & Schönberner, D. 1991, A&A, 240, L11
Borkowski, K. J., Sarazin, C. L., & Soker, N. 1990, ApJ, 360, 173
Dickey, J. M., & Lockman, F. J. 1990, ARA&A, 28, 215
Ferrière, K. M. 1995, ApJ, 441, 281
Frank, A., & Mellama, G. 1994, ApJ, 430, 800
Gaustad, J. E., & van Buren, D. 1993, PASP, 105, 1127
Grewing, M., & Bianchi, L. 1988, in A Decade of UV Astronomy with the *IUE* Satellite, Vol. 2, ed. E. J. Rolfe (Paris: ESA), 177
Hall, R. G. 1953, PASP, 65, 154
Heckathorn, J., Fesen, R. A., & Gull, T. P. 1982, A&A, 114, 414
Higdon, J. C., & Lingenfelter, R. E. 1980, ApJ, 239, 867
Holberg, J. B., Saffer, R. A., Tweedy, R. W., & Barstow, M. A. 1995, ApJ, 452, L133
Hollis, J. M., van Buren, D., Vogel, S. N., Feibelman, W. A., Jacoby, G. H., & Pedelty, J. A. 1996, ApJ, 456, 644
Ishida, K., & Weinberger, R. 1987, A&A, 178, 227
Jacoby, G. H. 1981, ApJ, 244, 903
Jacoby, G., & van de Steene, G. 1995, AJ, 110, 1285
Jasniewicz, G., Lapierre, G., & Monier, R. 1994, A&A, 287, 591
Jenkins, E. B. 1978, ApJ, 219, 845
Kwitter, K. B., Downes, R. A., & Chu, Y.-H. 1996, in preparation
Kwitter, K. B., Jacoby, G. H., & Lawrie, D. G. 1983, PASP, 95, 732
Kwitter, K. B., Jacoby, G. H., & Lydon, T. J. 1988, AJ, 96, 997
Kwitter, K. B., Massey, P., Congdon, C. W., & Pasachoff, J. M. 1989, AJ, 97, 1423
Liebert, J. W., Bergeron, P., & Tweedy, R. W. 1994, ApJ, 424, 817
Liebert, J. W., Green, R., Bond, H. E., Holberg, J. B., Wesemael, F., Fleming, T. A., & Kidder, K. 1989, ApJ, 346, 251
Livio, M. 1993, in IAU Symp. 155, Planetary Nebulae, ed. R. Weinberger & A. Acker (Dordrecht: Reidel), 279
Longmore, A. J., & Tritton, S. B. 1980, MNRAS, 193, 521
Marsh, T. R., Dhillon, V., & Duck, S. 1995, MNRAS, 275, 828
McKee, C. F. 1987, in Interstellar Processes, ed. D. J. Hollenbach & H. A. Thronson, Jr. (Dordrecht: Reidel), 237
McKee, C. F., Hollenbach, D. J., Seab, C. G., & Tielens, A. G. G. M. 1987, ApJ, 318, 674
Mellema, G. 1993, Ph.D. thesis, Univ. Leiden
Motch, C., Werner, K., & Pakull, M. W. 1993, A&A, 268, 561
Napiwotzki, R. 1993, Ph.D. thesis, Univ. Kiel
Napiwotzki, R., & Schönberner, D. 1993, in IAU Symp. 155, Planetary Nebulae, ed. R. Weinberger & A. Acker (Dordrecht: Reidel), 495
Plait, P., & Soker, N. 1990, AJ, 99, 1883
Purgathofer, A., & Weinberger, R. 1980, A&A, 87, L5
Shelton, R. L., & Cox, D. P. 1994, ApJ, 434, 599
Slavin, J. D., & Cox, D. P. 1993, ApJ, 417, 187
Soker, N. 1994, MNRAS, 270, 774
Spitzer, L. 1990, ARA&A, 28, 71
Tweedy, R. W., & Kwitter, K. B. 1994a, AJ, 108, 188
———. 1994b, ApJ, 433, L93
Tweedy, R. W., Martos, M., & Noriega-Crespo, A. C. 1995, ApJ, 447, 257
Tweedy, R. W., & Napiwotzki, R. 1994, AJ, 108, 978
Werner, K. 1993, in White Dwarfs: Advances in Observation and Theory, ed. M. A. Barstow (Dordrecht: Kluwer), 67
Werner, K., Heber, U., & Hunger, K. 1991, A&A, 244, 437